

THERMODYNAMIC RE-ASSESSMENT OF THE Al-Sn-Zn TERNARY SYSTEM

T. Cheng and L.-J. Zhang*

* State Key Laboratory of Powder Metallurgy, Central South University, Changsha, China

(Received 20 March 2019; accepted 27 June 2019)

Abstract

In this paper, a thermodynamic re-assessment of the Al-Sn-Zn ternary system was performed by means of the CALculation of PHase Diagram (CALPHAD) approach. The thermodynamic descriptions of the binary Al-Sn, Al-Zn, and Sn-Zn systems from the literature were directly adopted, and the newly reported experimental phase equilibria, enthalpies of mixing, and activities of Al in the ternary liquid phase were taken into account. A set of self-consistent thermodynamic parameters for the ternary Al-Sn-Zn system were finally obtained. A comprehensive comparison between the presently calculated phase equilibria/thermodynamic properties and the experimental data indicates that the present thermodynamic descriptions of the ternary Al-Sn-Zn system show very good agreement with most of the experimental data. The further direct comparison with the calculated results due to the previous assessment demonstrates that a significant improvement was achieved by the present assessment though fewer ternary interaction parameters were utilized.

Keywords: Al-Sn-Zn ternary system; CALPHAD; Thermodynamic assessment; Phase equilibrium

1. Introduction

The alloy systems containing lead (Pb) have been generally used as solders in electronics due to their low cost, superior mechanical properties, and excellent physical and chemical performances [1]. However, the Pb containing materials have been restricted by legislation worldwide because of their harmfulness to the environment and human health [2, 3]. In the recent years, development of the lead-free solder materials has attracted more attention among researchers [4-10]. To replace conventional Pb-Sn solders, the new lead-free solders should meet some requirements, such as the excellent electrical conductivity, optimal melting temperature, as well as good wetting joining surfaces [11]. Additional properties of the solder materials, such as high strength, corrosion resistance, and low cost have to be considered in design of the new lead-free solders [12, 13]. Among all the lead-free candidates, the melting temperature of Sn-Zn system (472.15 K) is very close to the eutectic temperature of Sn-Pb (456.15 K) [14]. In addition, the Sn-Zn solders have better mechanical strength than the conventional Sn-Pb solders [15]. However, Zn is well known for the problems related to wettability and corrosion and is very prone to oxidation [16]. The addition of aluminum can improve the corrosion resistance of the binary Sn-Zn alloys, even with very small amounts [17]. Therefore,

the ternary Al-Sn-Zn system is considered as an important candidate in the lead-free solder systems. In order to promote the development of the lead-free solders, knowledge of the phase equilibria and thermodynamic properties of the ternary Al-Sn-Zn system is of fundamental importance and indispensable for design of the novel solders in the framework of the CALculation of PHase Diagram (CALPHAD) approach [18, 19].

Until now, only Fries et al. [20] performed a thermodynamic assessment of the Al-Sn-Zn ternary system using the CALPHAD approach. Their thermodynamic descriptions have been included in the COST 507 database [21]. Moreover, the new experimental enthalpies of mixing of the ternary liquid phase, activities of Al in the liquid phase and phase equilibria data along different sections were reported recently [22-27]. Hence, it is necessary to re-assess the Al-Sn-Zn ternary system in order to construct the self-consistent thermodynamic database for the quaternary and higher-order lead-free systems. Moreover, there are three sub-binary systems i.e. Al-Sn, Al-Zn, and Sn-Zn in the Al-Sn-Zn ternary system. The Al-Sn binary system was first assessed by Fries et al. [20]. Later, Kang and Pelton [28] re-assessed the Al-Sn binary system by modeling the liquid phase with the modified quasi-chemical model (MQM). However, neither of the two groups [20, 28] considered the solubility of Sn in (Al)_{fcc} during their

*Corresponding author: lijun.zhang@csu.edu.cn



thermodynamic assessments. Furthermore, the new experimental data on enthalpies of mixing of the Al-Sn binary liquid phase were recently reported by Flandorfer et al. [29]. Hence, Cheng et al. [30] thermodynamically re-assessed the Al-Sn binary system by considering the solubility of Sn in $(Al)_{fcc}$, as well as the new experimental enthalpies of mixing in the liquid phase. The calculated results by Cheng et al. [30] showed better agreement with more experimental information than those in the previous assessment [20, 28]. Therefore, the thermodynamic parameters from Cheng et al. [30] were directly utilized in the present work. The Al-Zn binary system was first assessed by Murray [31]. However, the calculated phase diagram was not in good agreement with the experimental data available in the literature. Later, Mey and Effenberg [32] re-assessed this system, but the calculated phase boundaries of the $(Al)_{fcc}$ in the two-phase region ($(Al)_{fcc} + (Zn)_{hcp}$) and those for the miscibility gap of the $(Al)_{fcc}$ were different from the experimental data in the literature. After that, a thermodynamic assessment of this system was again performed by Mey [33], Chen and Chang [34], and Mathon et al. [35]. The three thermodynamic assessments gave very similar results. Recently, Wasiur-Rahman and Medraj [36] re-optimized the Al-Zn system with MQM. The thermodynamic descriptions of Al-Zn system reported by Mey [33] was used to establish the thermodynamic databases for the Al-Mg-Zn [37], Al-Cu-Zn [38], and Al-Zn-Ti [39] systems. In consideration of the compatibility of thermodynamic database in multi-component systems, the thermodynamic parameters of the Al-Zn system from Mey [33] were adopted in the present work, while the Sn-Zn binary system was thermodynamically assessed by several other authors [40-42]. It should be noted that Lee [40] assessed the Sn-Zn binary system based on more experimental data. The calculated results by Lee [40] show good agreement with most of the experimental data. Thus, the thermodynamic description by Lee [40] was adopted in the present work. The calculated phase diagrams of the Al-Sn, Al-Zn, and Sn-Zn binary systems from Refs. [30, 33, 40] are shown in Fig. 1.

Consequently, a CALPHAD re-assessment of the Al-Sn-Zn ternary system is to be performed by considering all the experimental data available in the literature and also the newly updated thermodynamic descriptions of boundary binaries. An accurate set of thermodynamic descriptions of the ternary Al-Sn-Zn system will be then established for the future development of the new Sn-Zn-Al-based solders.

2. Literature review

All the experimental phase equilibria and thermodynamic properties of the Al-Sn-Zn ternary

system available in the literature are strictly reviewed, and also concisely summarized in Table 1.

The liquidus temperatures of the Al-Sn-Zn ternary system over the entire concentration triangle were initially investigated by Plumbridge [43] using thermo analysis (TA). Afterwards, the liquidus surface of the Al-Sn-Zn ternary system was studied again by several authors [44-46] using TA. In 1980s, Vincent [47], Vincent and Sebaoub [48], and Vincent [49] experimentally studied several vertical sections (i.e., $Al_xSn_{1-x}-Sn_yZn_{1-y}$ and $Al_xZn_{1-x}-Sn$) in the Al-Sn-Zn ternary system using differential thermal analysis (DTA). Besides, Lin et al. [22] investigated the cooling curves of the Al-Sn-Zn solders with different compositions by measuring the temperature variations using thermocouple. In 2011, Sidorov et al. [23] studied the physical properties (i.e., density, electrical resistivity, and magnetic susceptibility) of the Al-Sn-Zn alloys at high temperatures. Moreover, liquidus temperatures of the several ternary Al-Sn-Zn alloy samples were also reported in Ref. [23]. In 2012, Smetana et al. [24] smelted 20 different Al-Sn-Zn alloys and measured their phase transition temperatures (including liquidus, solidus, and invariant reactions) using DTA. Recently, Drápala et al. [25] experimentally investigated the multiple Al-Sn-Zn alloys with various contents of elements. The phase transition temperatures (like liquidus, solidus, and invariant reactions) of these samples were determined by means of DTA method. Besides, the microstructures of partial sample were also studied by optical metallography (OM) and energy dispersive X-ray spectroscopy (EDX). All the experimental data in Refs. [22-25, 43-49] were employed in the present optimization.

The chemical potentials of Al in the Al-Sn-Zn liquid phase at 973 K and 1073 K along the $Sn_{0.5}Zn_{0.5}-Al$ join were experimentally determined by Tikhomirov and Sryvalin [50] using the electromotive force (EMF) method. In 2002, the enthalpies of mixing and activities of Al in the ternary liquid Al-Sn-Zn alloys at 973 K along different vertical sections (i.e., $Sn_{0.33}Zn_{0.66}-Al$, $Sn_{0.5}Zn_{0.5}-Al$ and $Sn_{0.66}Zn_{0.33}-Al$) were measured by Knnot and Mikula [26] using the EMF method. However, the enthalpies of mixing reported by Ref. [26] were not directly measured, but evaluated from the EMF values. In order to perform direct determination of the experimental data, the enthalpies of mixing of the liquid at 973 K along $Sn_{0.33}Zn_{0.66}-Al$, $Sn_{0.5}Zn_{0.5}-Al$ and $Sn_{0.66}Zn_{0.33}-Al$ joins were again investigated by Knnot et al. [27] by means of calorimetric method. Hence, the enthalpies of mixing of the ternary liquid phase from Ref. [27] were taken into account during optimization of the thermodynamic parameters, while the enthalpies of mixing by Knnot and Mikula [26] were **not**.



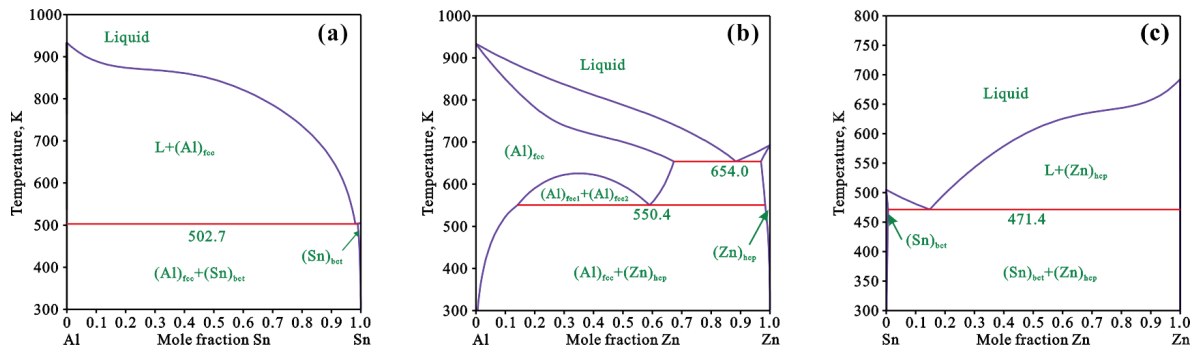


Figure 1. Calculated phase diagrams of (a) Al-Sn, (b) Al-Zn, and (c) Sn-Zn binary systems by Cheng et al. [30], Mey [33] and Lee [40], respectively

Table 1. Summary of all the experimental information of the ternary Al-Sn-Zn system available in the literature

Type of data	Experimental method	Reference
Phase equilibria data		
<u>Vertical sections</u>		
Al _{0.1131} Zn _{0.8869} ---Sn	Thermocouple	[22]
Al _{0.1198} Sn _{0.8802} ---Al _{0.0697} Zn _{0.9303}	DTA	[23-25]
Al _{0.0216} Sn _{0.9784} ---Al _{0.012} Zn _{0.988}	DTA	[24]
Al _{0.0425} Sn _{0.9575} ---Al _{0.0239} Zn _{0.9761}	DTA	[24]
Al _{0.0668} Sn _{0.9332} ---Al _{0.0379} Zn _{0.9621}	DTA	[24]
Al _{0.0746} Sn _{0.9254} ---Al _{0.0425} Zn _{0.9575}	DTA	[24]
Al _{0.902} Sn _{0.098} ---Sn _{0.098} Zn _{0.902}	DTA	[25]
Al _{0.8} Sn _{0.2} ---Sn _{0.2} Zn _{0.8}	DTA	[25]
Al _{0.6} Sn _{0.4} ---Sn _{0.4} Zn _{0.6}	DTA	[25]
Sn _{0.949} Zn _{0.051} ---Al	TA	[43]
Al _{0.4852} Zn _{0.5148} ---Sn	DTA	[47]
Al _{0.9754} Sn _{0.0246} ---Sn _{0.0577} Zn _{0.9423}	TA/DTA	[43-46, 48, 49]
Al _{0.6534} Sn _{0.3466} ---Sn _{0.5624} Zn _{0.4376}	TA/DTA	[43-45, 48]
<u>Isothermal sections</u>		
Liquid---(Al) _{fcc} ---(Zn) _{hcp}	OM and EDX	[25]
Thermodynamic properties		
Enthalpies of mixing in liquid		
Sn _{0.33} Zn _{0.67} ---Al	Calorimeter	[27]
Sn _{0.5} Zn _{0.5} ---Al	Calorimeter	[27]
Sn _{0.67} Zn _{0.33} ---Al	Calorimeter	[27]
Activities of Al in liquid		
Sn _{0.33} Zn _{0.67} ---Al	EMF	[26]
Sn _{0.5} Zn _{0.5} ---Al	EMF	[26]
Sn _{0.67} Zn _{0.33} ---Al	EMF	[26]
Chemical potentials of Al in liquid		
Sn _{0.5} Zn _{0.5} ---Al	EMF	[50]

TA = Thermal analysis; DTA = Differential thermal analysis; OM = Optical metallography; EDX = Energy dispersive X-ray spectroscopy; EMF = Electromotive force.

In the ternary Al-Sn-Zn system, there is one ternary eutectic reaction (L↔(Al)_{fcc}+(Sn)_{bcc}+(Zn)_{hcp}) and one ternary peritectic reaction (L+(Al)_{fcc2}↔(Al)_{fcc1}+(Zn)_{hcp}). The temperature and

phase compositions of the eutectic reaction were initially measured to be 469.15 K, 3.27 at.% Al and 10.60 at.% Sn by Plumbridge [43]. Afterwards, the temperature and phase compositions of the eutectic



reaction were again determined by Refs. [22, 24, 25, 43, 45-49, 51-53]. In the peritectic reaction, the $(Al)_{fcc1}$ represents the solid solution with high Al content, while the $(Al)_{fcc2}$ represents the solid solution with low Al content. Several groups [22, 24, 25, 47, 49, 52, 53] reported the temperature of the peritectic reaction. All experimental data of the two invariant reactions in the Al-Sn-Zn system are summarized in Table 3.

3. Thermodynamic models

The thermodynamic parameters of pure elements Al, Sn, and Zn were directly taken from SGTE compilation by Dinsdale [54]. The liquid and $(Al)_{fcc}$ phases were modeled as the completely disordered solution. Thus, the molar Gibbs energy of ϕ phase (ϕ = liquid, or $(Al)_{fcc}$) can be expressed as follows:

$$G_m^\phi = \sum_i x_i {}^0G_i^\phi + RT \sum_i x_i \ln x_i + {}^E G_m^\phi \quad (1)$$

where R is the gas constant, T is the absolute temperature, ϕ is the indicator of the liquid phase, x_i and ${}^0G_i^\phi$ are the mole fraction and the molar Gibbs energy of the elements i ($i=Al, Sn$ and Zn), and ${}^E G_m^\phi$ represents the excess Gibbs energy, which can be expressed by Redlich-Kister polynomial:

$${}^E G_m^\phi = \sum_i \sum_{j>i} x_i x_j \sum_{v=0}^n L_{i,j}^\phi (x_i - x_j)^v + \sum_i \sum_{j>i} \sum_{k>j} x_i x_j x_k (x_i {}^0L_{i,j,k}^\phi + x_j {}^1L_{i,j,k}^\phi + x_k {}^2L_{i,j,k}^\phi) \quad (2)$$

where $L_{i,j}$ and $L_{i,j,k}$ are the binary and ternary interaction parameters, respectively. The interaction parameter can be expressed in turn as the linear function of temperature, i.e., $a+bT$, with the coefficients a and b to be optimized.

4. Results and discussion

In the present work, the thermodynamic parameters of the ternary Al-Sn-Zn system were optimized through the PARROT module [55] incorporated in Thermo-Calc software package on the basis of the available experimental data from the literature. The principle of the optimization is based on the minimizing square sum of the differences between the measured and calculated values. During the optimization, each piece of experimental data was firstly given a fixed weight. Then, the weights were changed systematically during the optimization until most of the selected experimental data can be reproduced in the limits of the set uncertainty. In the first step of the assessment, only the enthalpies of mixing in the liquid phase from different vertical sections were considered to determine the ternary

interaction parameters (especially for a values) for the liquid phase. Secondly, the activities and chemical potentials of Al in the ternary Al-Sn-Zn liquid alloys were considered. The obtained ternary parameters for the liquid phase in the first step were then modified. Finally, the ternary interaction parameters for liquid phase have been optimized by the experimental phase equilibria information related to liquid phase. In addition, the contribution to Gibbs energy of the $(Al)_{fcc}$ solid solution phase from the Zn-Sn binary system is missing, because the $(Sn-Zn)_{fcc}$ phase is thermodynamically unstable. Hence, the $G_{Sn,Zn:Va}^{0,(Al)_{fcc}} = +20000$ was set and fixed to avoid the existence of the unstable $(Sn-Zn)_{fcc}$ phase during the optimization. A self-consistent set of thermodynamic parameters of the ternary Al-Sn-Zn system were finally obtained by considering all the experimental data, and they are listed in Table 2.

The calculated vertical sections in the ternary Al-Sn-Zn system using the presently established thermodynamic descriptions are shown in Figs. 2 to 9, compared with the experimental data by Refs. [22-27, 43-50]. Figure 2 presents the calculated vertical sections along $Al_xSn_{1-x}-Al_yZn_{1-y}$ (i.e., $Al_{0.0216}Sn_{0.9784}-Al_{0.012}Zn_{0.988}$, $Al_{0.0425}Sn_{0.9575}-Al_{0.0239}Zn_{0.9761}$, $Al_{0.0668}Sn_{0.9332}-Al_{0.0379}Zn_{0.9621}$ and $Al_{0.0746}Sn_{0.9254}-Al_{0.0425}Zn_{0.9575}$) close to the Sn-Zn side, compared with the experimental data by Ref. [24]. Moreover, the calculated results due to the previous thermodynamic assessment by Fries et al.

Table 2. Summary of the thermodynamic parameters in the Al-Sn-Zn ternary system finally obtained in the present work and from the literature

Phase	Thermodynamic parameters	Reference
Liquid (Al, Sn, Zn) ₁	$G_{Al,Sn}^{0,L} = +15713.581 - 4.136T$	[30]
	$G_{Al,Sn}^{1,L} = +4017.05 - 0.936T$	[30]
	$G_{Al,Sn}^{2,L} = +2051.11 - 0.2685T$	[30]
	$G_{Al,Zn}^{0,L} = +10465.55 - 3.39259T$	[33]
	$G_{Sn,Zn}^{0,L} = +12558 - 8.7041T$	[40]
	$G_{Sn,Zn}^{1,L} = -5623 + 4.196T$	[40]
	$G_{Sn,Zn}^{2,L} = +4149 - 4.091T$	[40]
	$G_{Al,Sn,Zn}^{0,L} = 0$	This work
	$G_{Al,Sn,Zn}^{1,L} = +12768.22 - 21.165T$	This work
$G_{Al,Sn,Zn}^{2,L} = -2000 + 22.20T$	This work	
$(Al)_{fcc}$ (Al, Sn, Zn) ₁ (Va) ₁	$G_{Al,Sn:Va}^{0,(Al)_{fcc}} = +76777.656 - 28.499T$	[30]
	$G_{Al,Zn:Va}^{0,(Al)_{fcc}} = +7297.48 + 0.47512T$	[33]
	$G_{Al,Zn:Va}^{1,(Al)_{fcc}} = +6612.88 - 4.5911T$	[33]
	$G_{Al,Zn:Va}^{2,(Al)_{fcc}} = -3097.19 + 3.30635T$	[33]
	$G_{Sn,Zn:Va}^{0,(Al)_{fcc}} = +20000$	This work



[20] are also superimposed in the plots for a direct comparison. The solid blue lines represent the calculated results in the present work, while the red dashed lines are from Fries et al. [20]. As shown in Fig. 2, most of the experimental data can be well reproduced by the present thermodynamic modeling. Furthermore, a significant improvement can be clearly observed, compared with the previous one [20]. Figure 3 gives the comparison between the calculated vertical sections (i.e., $Al_{0.1198}Sn_{0.8802}$ —

$Al_{0.0697}Zn_{0.9303}$ and $Sn_{0.949}Zn_{0.051}$ —Al) with the experimental data by Refs. [23-25, 43] and the calculated results due to the previous assessment by Fries et al. [20]. As shown in Fig. 3 (a), the calculated result shows a good agreement with most of the experimental data [23-25]. Compared with the previous one [20], the present work can better reproduce the experimental data [23-25]. Similarly, Fig. 3(b) shows the presently calculated result is in good agreement with the experimental data [43] and

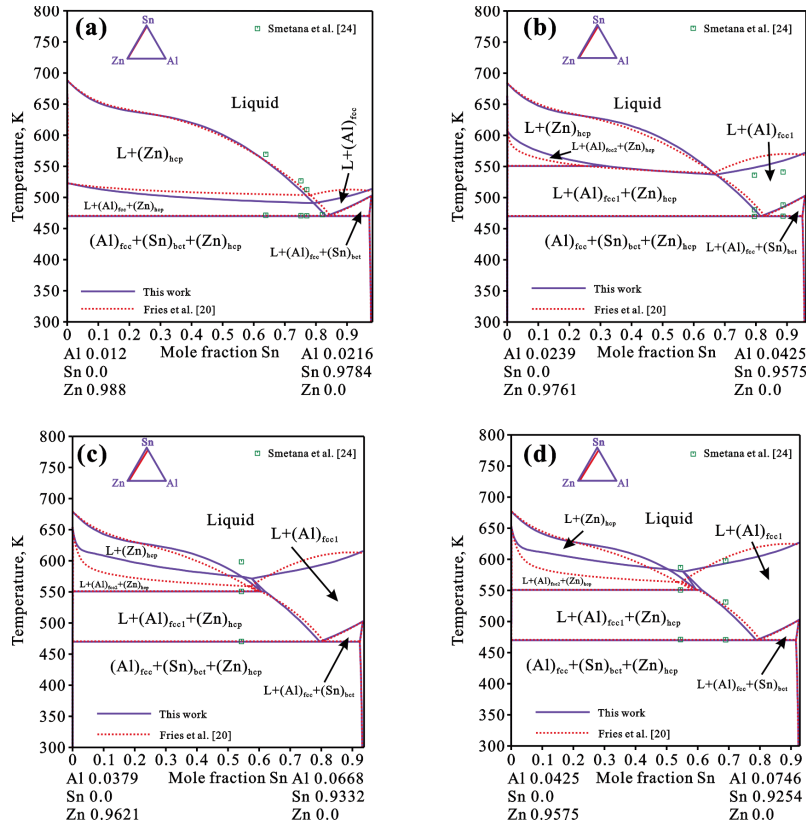


Figure 2. Calculated vertical sections along $Al_{x}Sn_{1-x}$ — $Al_{y}Zn_{1-y}$ joins, compared with the experimental data [24] and the previous assessment [20]: (a) $Al_{0.0216}Sn_{0.9784}$ — $Al_{0.012}Zn_{0.988}$ (b) $Al_{0.0425}Sn_{0.9575}$ — $Al_{0.0239}Zn_{0.9761}$ (c) $Al_{0.0668}Sn_{0.9332}$ — $Al_{0.0379}Zn_{0.9621}$ and (d) $Al_{0.0746}Sn_{0.9254}$ — $Al_{0.0425}Zn_{0.9575}$

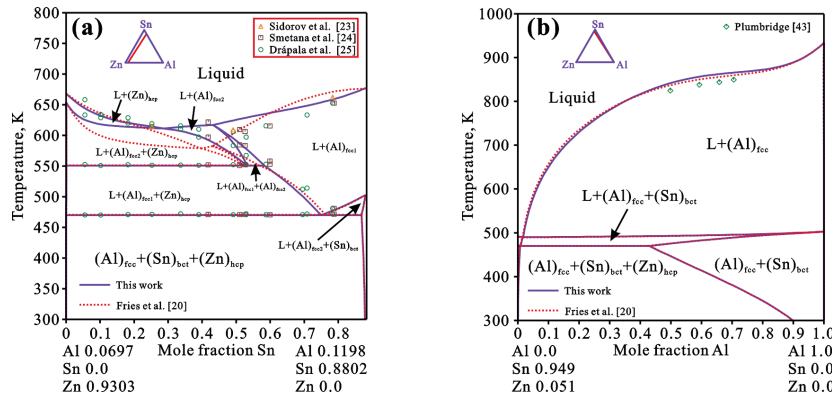


Figure 3. Calculated vertical sections along (a) $Al_{0.1198}Sn_{0.8802}$ — $Al_{0.0697}Zn_{0.9303}$ and (b) $Sn_{0.949}Zn_{0.051}$ —Al, compared with the experimental data [23-25, 43] and the previous assessment [20]



also the previous assessment [20]. The vertical sections along the $\text{Al}_{0.1131}\text{Zn}_{0.8869}\text{—Sn}$ and $\text{Al}_{0.4852}\text{Zn}_{0.5148}\text{—Sn}$ joins were calculated and displayed in Fig. 4. As shown in Fig. 4(a), the experimental data [22] can be well reproduced by the present thermodynamic calculations. A meaningful improvement is achieved in comparison with the previous assessment by Fries et al. [20]. However, Fig. 4(b) shows some deviations between the present calculation and the calculation based on the previous assessment by Fries et al. [20] and the experimental data [47], which exist in the liquidus. As shown in Fig. 4(b), the largest deviation is located around 40–70 at.% Sn. One of the possible reasons for such deviation is that the mass loss of Sn occurred during the experimental melting process for the alloys with high content of Sn. Therefore, further accurate experiments are necessary for validation. Figure 5 shows the calculated vertical sections along $\text{Al}_{0.9754}\text{Sn}_{0.0246}\text{—Sn}_{0.0577}\text{Zn}_{0.9423}$ and $\text{Al}_{0.6534}\text{Sn}_{0.3466}\text{—Sn}_{0.5624}\text{Zn}_{0.4376}$, in comparison with the experimental data [43–46, 48, 49] and also the previous assessment [20]. The presently calculated results are in good

agreement with the experimental data [43–46, 48, 49] and the calculated results by Fries et al. [20]. Figure 6 presents the calculated vertical sections along $\text{Al}_{0.902}\text{Sn}_{0.098}\text{—Sn}_{0.098}\text{Zn}_{0.902}$, $\text{Al}_{0.8}\text{Sn}_{0.2}\text{—Sn}_{0.2}\text{Zn}_{0.8}$ and $\text{Al}_{0.6}\text{Sn}_{0.4}\text{—Sn}_{0.4}\text{Zn}_{0.6}$ joins, respectively. Again, as can be seen, the presently calculated results agree well with the experimental data [25], and also the previous assessment by Ref. [20].

Figure 7 shows the calculated enthalpies of mixing of the ternary Al–Sn–Zn liquid phase (reference states: liquid Al, liquid Sn and liquid Zn) at 973 K along the $\text{Sn}_{0.33}\text{Zn}_{0.67}\text{—Al}$, $\text{Sn}_{0.5}\text{Zn}_{0.5}\text{—Al}$, and $\text{Sn}_{0.67}\text{Zn}_{0.33}\text{—Al}$ joins, compared with the experimental data [27] and the calculated results due to the previous assessment by [20]. The presently calculated results show perfect agreement with all the measured experimental data [27]. Furthermore, there is a significant improvement, compared with the calculated results by [20], especially close to the Sn–Zn boundary binary. Figure 8 represents the calculated activities of Al (reference state: liquid Al) in the ternary Al–Sn–Zn liquid alloys at 973 K, compared with the experimental data [26] and also the calculated results due to the previous

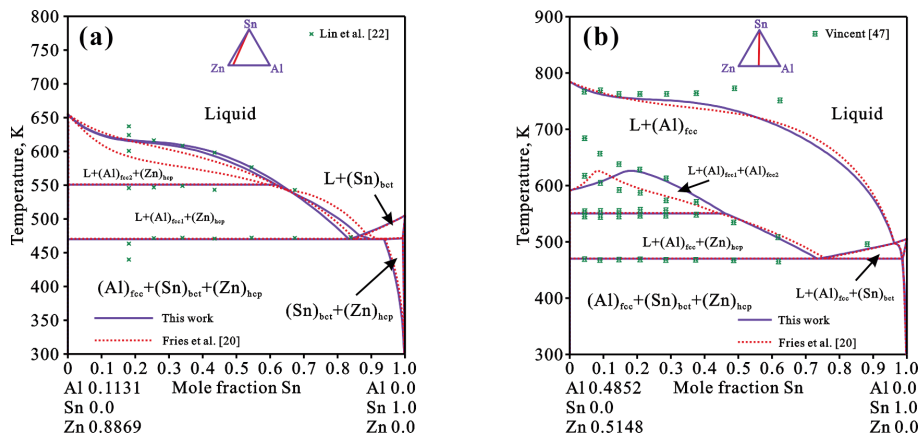


Figure 4. Calculated vertical sections along (a) $\text{Al}_{0.1131}\text{Zn}_{0.8869}\text{—Sn}$ and (b) $\text{Al}_{0.4852}\text{Zn}_{0.5148}\text{—Sn}$, compared with the experimental data [22, 47] and the previous assessment [20]

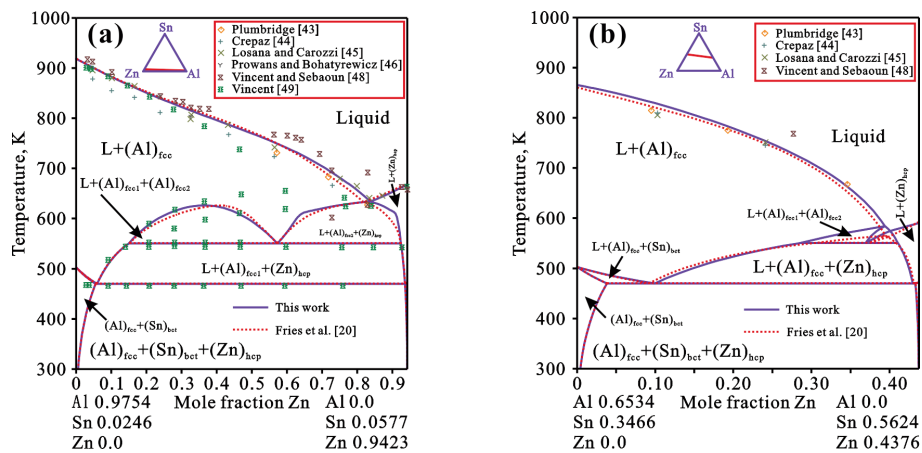


Figure 5. Calculated vertical sections along (a) $\text{Al}_{0.9754}\text{Sn}_{0.0246}\text{—Sn}_{0.0577}\text{Zn}_{0.9423}$ and (b) $\text{Al}_{0.6534}\text{Sn}_{0.3466}\text{—Sn}_{0.5624}\text{Zn}_{0.4376}$ compared with the experimental data [43–46, 48, 49] and the previous assessment [20]



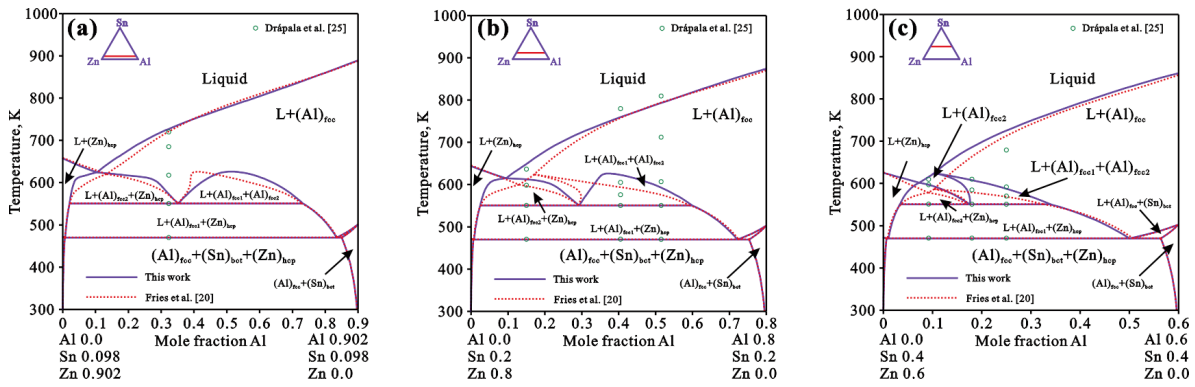


Figure 6. Calculated vertical sections along $Al_{1-x}Sn_x-Zn_{1-x}$ joins, compared with the experimental data [25] and the previous assessment [20]: (a) $Al_{0.902}Sn_{0.098}-Sn_{0.098}Zn_{0.902}$, (b) $Al_{0.8}Sn_{0.2}-Sn_{0.2}Zn_{0.8}$ and (c) $Al_{0.6}Sn_{0.4}-Sn_{0.4}Zn_{0.6}$.

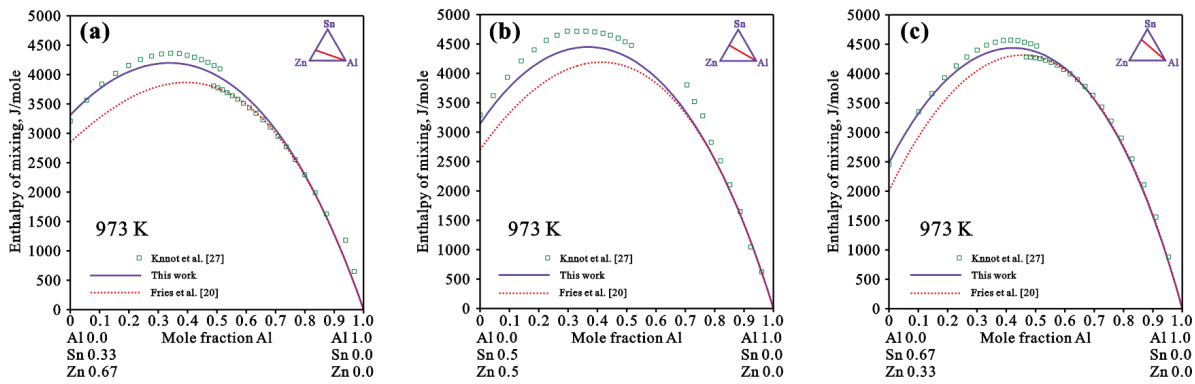


Figure 7. Calculated enthalpies of mixing of the ternary liquid phase at 973 K along (a) $Sn_{0.33}Zn_{0.67}-Al$, (b) $Sn_{0.5}Zn_{0.5}-Al$ and (c) $Sn_{0.67}Zn_{0.33}-Al$, compared with the experimental data [27] and the previous assessment [20]. The reference states are liquid Al, liquid Sn and liquid Zn

assessment by [20]. As can be seen, the presently calculated results agree well with the experimental data [26], and also the calculated results by Fries et al. [20]. Figures 9(a) and (b) display the calculated chemical potentials of Al (reference state: liquid Al) in the ternary Al-Sn-Zn liquid alloys at 973 K and 1073 K, respectively. It should be noted that most of the experimental data [50] can be well reproduced by the present thermodynamic calculations, which are also consistent with the previous assessment by Fries et al. [20].

Figures 10(a) and (b) represent the calculated isothermal sections of the ternary Al-Sn-Zn system at 523.15 K from the present work and the previous assessment [20], compared with the same experimental data [25]. In the plots, the alloys No. 1, 2, and 3 represent the initial components of experimental alloys. The No. 1', 2', and 3' represent the phase compositions of $(Al)_{fcc}$ after long-time homogenization of the alloys No. 1, 2, and 3, respectively, while the No. 1'', 2'', and 3'' represent the phase compositions of $(Zn)_{hcp}$. As can be seen, the calculated results from both the present work and the previous assessment [20] show perfect agreement with the experimental data by [25]. Similarly, Figs. 11(a) and (b) show the calculated isothermal sections of the ternary

Al-Sn-Zn system at 573.15 K from the present assessment and the previous one by Fries et al. [20], respectively. Again, the calculated results from both the present work and the previous assessment [20] can well reproduce the experimental data [25]

Figure 12 shows the calculated liquidus projection of the ternary Al-Sn-Zn system over the entire composition range (a) and in the Sn-rich corner (b) according to the presently obtained thermodynamic descriptions. As can be clearly seen in Fig. 12, there are three primary crystallization fields, i.e. $(Al)_{fcc}$, $(Sn)_{bcc}$, and $(Zn)_{hcp}$. The E_1 represents the eutectic reaction $(L \leftrightarrow (Al)_{fcc} + (Sn)_{bcc} + (Zn)_{hcp})$, while the U_1 represents the peritectic reaction $(L + (Al)_{fcc2} \leftrightarrow (Al)_{fcc1} + (Zn)_{hcp})$. Table 3 summarizes the invariant equilibria associated with the liquid phase in the ternary Al-Sn-Zn system from different sources. As can be clearly seen in Table 3, the calculated invariant reactions due to the present thermodynamic descriptions can reproduce all experimental data, which are in good agreement with each other. Furthermore, there is a critical point A in the liquidus projection. Such point A represent the start of separation of liquid into the $(Al)_{fcc1}$ and $(Al)_{fcc2}$ (i.e., $L \leftrightarrow (Al)_{fcc1} + (Al)_{fcc2}$) at 626.19 K with composition of 50.25 at.% Zn and 39.18 at.% Sn.



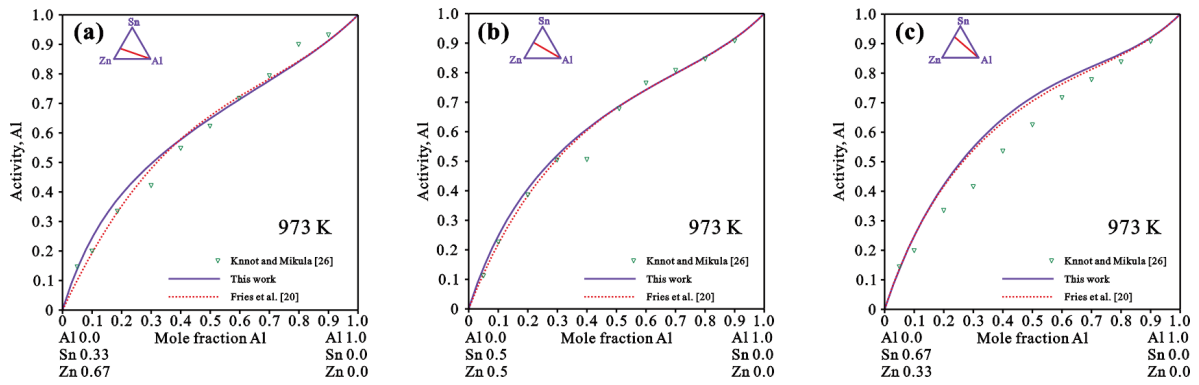


Figure 8. Calculated activities of Al in the ternary liquid phase at 973 K along (a) $Sn_{0.33}Zn_{0.67}-Al$, (b) $Sn_{0.5}Zn_{0.5}-Al$ and (c) $Sn_{0.67}Zn_{0.33}-Al$, compared with the experimental data [26] and the previous assessment [20]. The reference state is liquid Al

Table 3. Summary of the calculated invariant reactions of the ternary Al-Sn-Zn system, in comparisons with the experimental data in the literature

Invariant reaction	Type	T/K	Phase	Composition/at. %		Reference
				Sn	Zn	
$L \leftrightarrow (Al)_{fcc} + (Sn)_{bct} + (Zn)_{hcp}$	E_1	469.82 Calc.	L	83.81	14.74	This work
			$(Al)_{fcc}$	0	5.67	This work
			$(Sn)_{bct}$	98.64	0.64	This work
			$(Zn)_{hcp}$	0.03	99.36	This work
		469.15 Exp.	L	86.13	10.6	[43]
		469.15 Exp.	L	77.57	16.62	[45]
		470.45 Exp.	L	84.66	12.91	[46]
		471.15 Exp.	L	82.65	14.94	[51]
		470.66 Exp.	L			[22]
		470.79 Exp.	L			[24]
		470.82 Exp.	L			[25]
		467.84 Exp.	L			[47]
		470.15 Exp.	L			[48]
		470.15 Exp.	L			[49]
		470.15 Exp.	L			[52]
469.15 Exp.	L			[53]		
$L + (Al)_{fcc2} \leftrightarrow (Al)_{fcc1} + (Zn)_{hcp}$	U_1	550.57 Calc.	L	62.87	32.76	This work
			$(Al)_{fcc1}$	0	14.12	This work
			$(Al)_{fcc2}$	0.02	59.09	This work
			$(Zn)_{hcp}$	0.07	98.32	This work
		546.08 Exp.	L			[22]
		551.43 Exp.	L			[24]
		551.31 Exp.	L			[25]
		550.22 Exp.	L			[47]
		551.15 Exp.	L			[49]
		551.15 Exp.	L			[52]
548.15~549.15 Exp.	L			[53]		

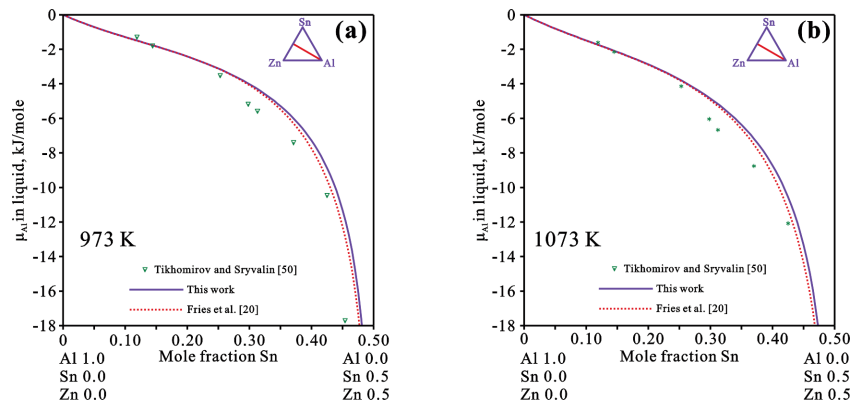


Figure 9. Calculated chemical potentials of Al in the ternary liquid phase along $Sn_{0.5}Zn_{0.5}-Al$ join, compared with the experimental data [50] and the previous assessment [20]: (a) 973 K and (b) 1073 K. The reference state is liquid Al.

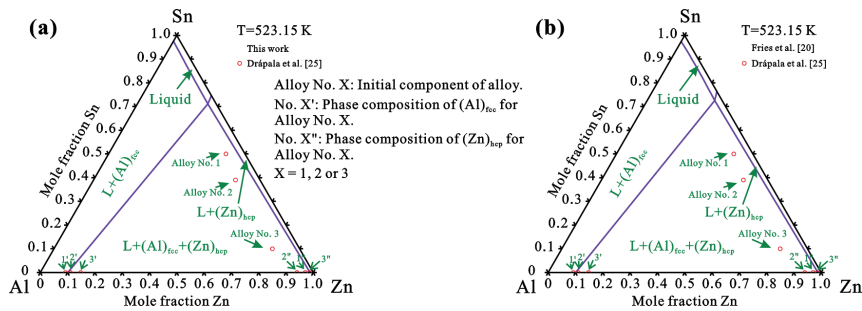


Figure 10. Calculated isothermal sections of the ternary Al-Sn-Zn system at 523.15 K due to: (a) the present thermodynamic descriptions and (b) the previous assessment [20], compared with the experimental data [25]

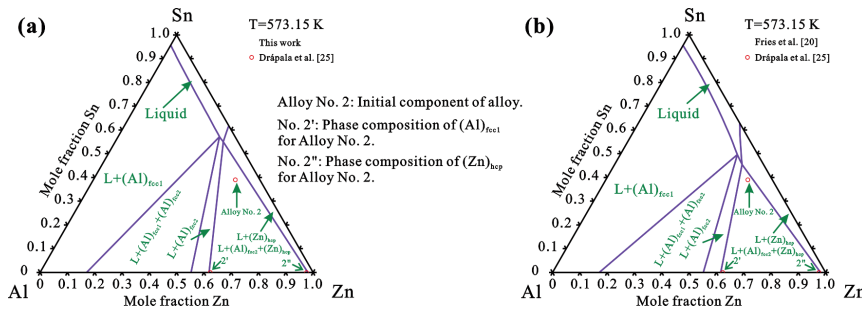


Figure 11 Calculated isothermal sections of the ternary Al-Sn-Zn system at 573.15 K due to: (a) the present thermodynamic descriptions and (b) the previous assessment [20], compared with the experimental data [25]

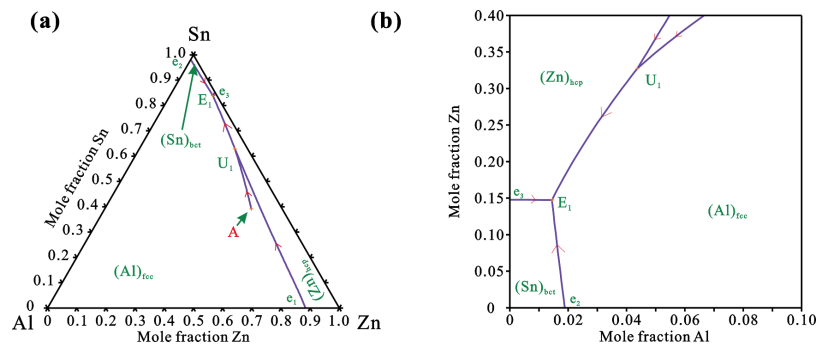


Figure 12. Calculated liquidus projection of the Al-Sn-Zn ternary system according to the present thermodynamic descriptions: (a) over the entire composition range, and (b) close to the Sn-rich corner



5. Conclusions

All the experimental phase equilibria and thermodynamic properties of the ternary Al-Sn-Zn system available in the literature were critically reviewed.

A CALPHAD-type thermodynamic assessment of the Al-Sn-Zn ternary system was performed by taking all the experimental data, and the thermodynamic descriptions for the boundary binaries into account. A set of self-consistent thermodynamic parameters of the Al-Sn-Zn ternary system was finally obtained.

Various phase equilibria and thermodynamic properties were calculated according to the obtained thermodynamic parameters, and comprehensively compared with the experimental data, and also the calculated results due to the previous assessment. The calculated results due to the present thermodynamic descriptions can reproduce most of the experimental data. Moreover, though with fewer ternary interaction parameters, a significant improvement was achieved in the present assessment, in comparison with the previous one.

Acknowledgments

The financial support from the National Key Research and Development Program of China (Grant No. 2016YFB0301101), the National Natural Science Foundation of China (Grant No. 51602351), and the Hunan Provincial Science and Technology Program of China (Grant No. 2017RS3002)-Huxiang Youth Talent Plan is acknowledged.

References

- [1] W. Gašior, Z. Moser, J. Pstruší, J. Phase Equilib., 22 (1) (2001) 20-25.
- [2] G. Böhm, H. R. Pfister, Acta Psychol., 104 (3) (2000) 317-337.
- [3] A. Kicińska, Chemosphere, 215 (2019) 574-585.
- [4] M. Xiong, L. Zhang, J. Mater. Sci., 54 (2) (2019) 1741-1768.
- [5] H. M. Henao, C. Chu, J. P. Solis, K. Nogita, Metall. Mater. Trans. B, 50 (1) (2019) 502-516.
- [6] S. Tian, S. Li, J. Zhou, F. Xue, J. Alloys Compd., 742 (2018) 835-843.
- [7] K. N. Reeve, C. A. Handwerker, J. Electron. Mater., 47 (1) (2018) 61-76.
- [8] R. M. Novaković, S. Delsante, G. Borzone, J. Min. Metall. Sect. B-Metall., 54 (2) (2018) 251-260.
- [9] M. Benke, Z. Salyi, G. Kaptay, J. Min. Metall. Sect. B-Metall., 54 (3) (2018) 283-290.
- [10] G. Chen, F. Wu, C. Liu, V. V. Silberschmidt, Y. C. Chan. J. Alloys Compd., 656 (2016) 500-509.
- [11] T. Laurila, V. Vuorinen, J. K. Kivilahti, Mater. Sci. Eng., 49 (1-2) (2005) 1-60.
- [12] N. Moelans, K. C. H. Kumar, P. Wollants, J. Alloys Compd., 360 (1-2) (2003) 98-106.
- [13] Y. A. Odusote, A. I. Popoola, S. S. Oluyamo. Appl. Phys. A: Mater., 122 (2) (2016) 80.
- [14] K. L. Lin, T. P. Liu. Oxid. Met., 50 (3-4) (1998) 255-267.
- [15] H. Maroori, S. Vaynman, J. Chin, B. Moran, L. M. Keer, M. E. Fine. Mat. Res. Soc. Symp. Proc., 390 (1995) 161-175.
- [16] T. Hofmann, N. Schuwirth. J. Soil Sediment, 8 (6) (2008) 433-441.
- [17] M. Kitajima, T. Kobayashi, M. Noguchi, T. Shono, K. Yamazaki, T. Ogino: International Conference on Lead Free Electronics, Conference Proceedings, June 11-12, Frankfurt, Germany, 2003, p. 211.
- [18] R. Shi, A. A. Luo. Calphad, 62 (2018) 1-17.
- [19] Z. Lu, L. Zhang. Mater. Design, 116 (2017) 427-437.
- [20] S. G. Fries, H. L. Lukas, S. Kuang, F. Hayes (Ed.). User Aspects of Phase Diagrams, The Institute of Metals, London, 1991, p. 280-286.
- [21] I. Ansara, A. T. Dinsdale, M. H. Rand (Ed.). COST 507, thermochemical database for light metal alloys, in: European Communities, Vol. 2, Belgium, 1998.
- [22] K. L. Lin, L. H. Wen, T. P. Liu. J. Electron. Mater., 27 (3) (1998) 97-105.
- [23] V. Sidorov, J. Drápala, S. Uporov, A. Sabirzyanov, P. Popel, A. Kurochkin, K. Grushevskij. Some physical properties of Al-Sn-Zn melts, in: EPJ Web of Conferences, 15 (2011) 01022.
- [24] B. Smetana, S. Zlá, A. Kroupa, M. Žaludová, J. Drápala, R. Burkovič, D. Petlák. J. Therm. Anal. Calorim., 110 (1) (2012) 369-378.
- [25] J. Drápala, G. Kostiuková, B. Smetana, M. Madaj, A. Kroupa. Adv. Sci. Eng. Med., 7 (4) (2015) 291-295.
- [26] S. Knott, A. Mikula. Mater. Trans., 43 (8) (2002) 1868-1872.
- [27] S. Knott, H. Flandorfer, A. Mikula. Z. Metallkd., 96 (1) (2005) 38-44.
- [28] Y. B. Kang, A. D. Pelton. Calphad, 34 (2) (2010) 180-188.
- [29] H. Flandorfer, M. Rechchach, A. Elmahfoudi, L. Bencze, A. Popovič, H. Ipsér. J. Chem. Thermodyn. 43 (11) (2011) 1612-1622.
- [30] T. Cheng, Y. Tang, L. Zhang. Calphad, 64 (2019) 354-363.
- [31] J. L. Murray. Bull. Alloy Phase Diagr. 4 (1) (1983) 55-73.
- [32] S. A. Mey, G. Effenberg. Z. Metallkd. 77 (7) (1986) 449.
- [33] S. A. Mey. Z. Metallkd. 84 (7) (1993) 451-454.
- [34] S. L. Chen, Y. A. Chang. Calphad, 17 (2) (1993) 113-124.
- [35] M. Mathon, K. Jardet, E. Aragon, P. Satre, A. Sebaoun. Calphad, 24 (3) (2000) 253-284.
- [36] S. Wasiur-Rahman, M. Medraj. Calphad, 33 (3) (2009) 584-598.
- [37] P. Liang, T. Tarfa, J. A. Robinson, S. Wagner, P. Ochin, M. G. Harmelin, H. J. Seifert, H. L. Lukas, F. Aldinger. Thermochim. Acta, 314 (1-2) (1998) 87-110.
- [38] S. M. Liang, R. Schmid-Fetzer. Calphad, 52 (2016) 21-37.
- [39] Q. Luo, Q. Li, J. Y. Zhang, S. L. Chen, K. C. Chou.



- Intermetallics, 33 (2013) 73-80.
- [40] B. J. Lee. Calphad, 20 (4) (1996) 471-480.
- [41] H. Ohtani, M. Miyashita, K. Ishida. J. Jpn. Inst. Met., 63 (6) (1999) 685-694.
- [42] C. Yang, F. Chen, W. Gierlotka, S. Chen, K. Hsieh, L. Huang. Mater. Chem. Phys., 112 (1) (2008) 94-103.
- [43] D. V. Plumbridge. On the Binary and Ternary Alloys of Al, Zn, Cd and Sn (In German). Thesis, University of München, Germany (1911).
- [44] E. Crepaz. Giorn. Chim. Ind. Appl., 6 (1923) 285-290.
- [45] L. Losana, E. Carozzi. Gazz. Chim. Ital., 53 (1923) 546-554.
- [46] S. Prowans, M. Bohatyrewicz. Arch. Hutn., 13 (1968) 217-233.
- [47] D. Vincent. Contribution to the Study of the Ternary Al-Zn-Sn System (In French). Thesis No. 84, Universite Claude Bernard, Lyon I, France, 1980.
- [48] D. Vincent, A. Sebaoun. J. Therm. Anal., 20 (1981) 419-433.
- [49] D. Vincent. Contribution to the Study of the Ternary Al-Zn-Sn System (In French). Thesis No. 81, Universite Claude Bernard, Lyon I, France, 1982.
- [50] A. A. Tikhomirov, I. T. Sryvalin. Sb. Nauch. Tr.-Perm. Politekh. Inst., 18 (1965) 193-198.
- [51] A. K. Nayak, Trans. Indian Inst. Met., 28 (1975) 285-90.
- [52] E. Aragon, A. Sebaoun, J. Therm. Anal. Calorim., 52 (2) (1998) 523-535.
- [53] E. Aragon, D. Vincent, A. Zahra A. Sebaoun, J. Therm. Anal. Calorim., 55 (1) (1999) 271-282.
- [54] A. T. Dinsdale. Calphad, 15 (4) (1991) 317-425.
- [55] B. Sundman, B. Jansson, J. O. Andersson. Calphad, 9 (2) (1985) 153-190.

TERMODINAMIČKA REOPTIMIZACIJA Al-Sn-Zn TROJNOG SISTEMA

T. Cheng i L.-J. Zhang*

*Glavna državna laboratorija za metalurgiju praha, Centralno – južni univerzitet, Čangša, Kina

Apstrakt

U ovom radu je izvršena termodinamička reoptimizacija Al-Sn-Zn trojnog sistema koristeći pristup proračuna faznog dijagrama (CALPHAD). Korišćene su termodinamičke optimizacije binarnih sistema Al-Sn, Al-Zn i Sn-Zn koje su dostupne u literaturi, a publikovani eksperimentalni rezultati koji se odnose na ispitivanja fazne ravnoteže, entalpije mešanja i aktivnosti Al u tečnoj fazi su takođe uzeti u obzir. Na kraju je dobijen set konzistentnih termodinamičkih parametara za Al-Sn-Zn trojni sistem. Sveobuhvatno poređenje proračunatih faznih ravnoteža i termodinamičkih osobina sa eksperimentalnim podacima pokazuje da je sadašnji termodinamički opis Al-Sn-Zn trojnog sistema u slaganju sa većinom eksperimentalnih podataka. Dalje direktno poređenje sa rezultatima proračuna iz prethodne optimizacije pokazuje da je postignut značajan napredak nakon nove optimizacije, iako je korišćeno manje parametara ternarne interakcije.

Ključne reči: Al-Sn-Zn trojni sistem; CALPHAD; Termodinamička optimizacija; Fazna ravnoteža

